X-ray Free Electron Laser-Induced Synthesis of ε-Iron Nitride at High Pressures

Huijeong Hwang,[a,ϕ] Taehyun Kim,[a] Hyunchae Cynn,[b] Thomas Vogt,[c] Rachel.J. Husband,[d] Karen Appel,[e] Carsten Baehtz,[e] Orianna B. Ball,[f] Marzena A. Baron,[g] Richard Briggs,[b] Maxim Bykov,[h] Elena Bykova,[h] Valerio Cerantola,[e] Julien Chantel,[i] Amy L. Coleman,[b] Dana Dattlebaum,[j] Leora E. Dresselhaus-Marais,[b] Jon H. Eggert,[b] Lars Ehm,[k] William J. Evans,[b] Guillaume Fiquet,[g] Mungo Frost,[l] Konstantin Glazyrin,[d] Alexander F. Goncharov,[h] Zsolt Jenei,[b] Jaeyong Kim,[m] Zuzana Konôpková,[e] Jona Mainberger,[d] Mikako Makita,[e] Hauke Marquardt,[n] Emma E. McBride,[l] James D. McHardy,[f] Sébastien Merkel,[i] Guillaume Morard,[g],[o] Earl F. O'Bannon III,[b] Christoph Otzen,[d] Edward J. Pace,[f] Alexander Pelka,[e] Charles M. Pépin,[p],[q] Jeffrey S. Pigott,[j],[r] Vitali B. Prakapenka,[s] Clemens Prescher,[d] Ronald Redmer,[t] Sergio Speziale,[u] Georg Spiekermann,[v] Cornelius Strohm,[d] Blake T. Sturtevant,[j] Nenad Velisavljevic,[b] Max Wilke,[v] Choong-Shik Yoo,[w] Ulf Zastrau,[e] Hanns-Peter Liermann,[d] Malcolm I. McMahon,[f] R. Stewart McWilliams,[f] Yongjae Lee*,[a]*

(EuXFEL Community Proposal #2292)

AUTHOR ADDRESS

[a] Earth System Sciences, Yonsei University, 50 Yonsei-ro, Seodaemun-gu, Seoul 03722, Republic of Korea

[b] Lawrence Livermore National Laboratory, 7000 East Avenue, Livermore, CA 94550, USA

[c] Nano Center and Department of Chemistry and Biochemistry, University of South Carolina, Columbia, South Carolina 29208, USA

[d] Photon Sciences, Deutsches Elektronen-Synchrotron (DESY), Notkestraße 85, Hamburg 22607, Germany

[e] European XFEL GmbH, Holzkoppel 4, 22869 Schenefeld, Germany

[f] The School of Physics and Astronomy, Centre for Science at Extreme Conditions and SUPA, University of Edinburgh, Peter Guthrie Tait Road, Edinburgh, EH9 3FD, UK

[g] Inst. Minéralogie, de Physique des Matériaux et de Cosmochimie (IMPMC), Sorbonne University, UMR CNRS 7590, Muse-um National d'Histoire Naturelle, 4 Place Jussieu, Paris, France

[h] Carnegie Science, Earth and Planets Laboratory, 5241 Broad Branch Road, NW, Washington, DC 20015

[i] Univ. Lille, CNRS, INRAE, Centrale Lille, UMR 8207 - UMET - Unité Matériaux et Transformations, F-59000 Lille, France

[j] Los Alamos National Laboratory, Los Alamos, New Mexico 87545, USA

[k] Mineral Physics Institute, Stony Brook University, Stony Brook, NY 11794, USA

[l] SLAC National Accelerator Laboratory, 2575 Sand Hill Road, Menlo Park, California 94025, USA

[m] Department of Physics, Research Institute for Natural Science, HYU-HPSTAR-CIS High Pressure Research Center, Hanyang University, 222 Wangsimni-ro, Seongdong-Ku, Seoul 04763, Republic of Korea

[n] Department of Earth Sciences, University of Oxford, South Parks Road, OX1 3AN Oxford, United Kingdom

[o] Université Grenoble Alpes, Université Savoie Mont Blanc, CNRS, IRD, IFSTTAR, ISTerre, 38000 Grenoble, France

[p] CEA, DAM, DIF, F-91297 Arpajon, France

[q] Université Paris-Saclay, Laboratoire Matière en Conditions Extrêmes, 91680 Bruyères-le-Châtel, France

[r] Case Western Reserve University, 10900 Euclid Ave, Cleveland, OH 44106, United States

[s] Center for Advanced Radiation Sources, University of Chicago, Chicago, IL 60637, USA.

[t] Universität Rostock, Institut für Physik, D-18051 Rostock, Germany

[u] GFZ German Research Centre for Geosciences, Telegrafenberg, 14473 Potsdam, Germany

[v] Institut für Geowissenschaften, Universität Potsdam, Karl-Liebknecht-Straße 24-25, 14476 Potsdam, Germany

[w] Department of Chemistry, Institute of Shock Physics, and Materials Science and Engineering, Washington State University, Pullman, Washington 99164, USA

ϕ Present address: Photon Sciences, Deutsches Elektronen-Synchrotron (DESY), Notkestraße 85, Hamburg 22607, Germany

* Correspondence to: yongjaelee@yonsei.ac.kr (Yongjae Lee) / rs.mcwilliams@ed.ac.uk (R. Stewart McWilliams)

ABSTRACT The ultrafast synthesis of ε-Fe_3N_{1+x} in a diamond-anvil cell (DAC) from Fe and N_2 under pressure was observed using serial exposures of an X-ray free electron laser (XFEL). When the sample at 5 GPa was irradiated by a pulse train separated by 443 ns, the estimated sample temperature at the delay time was above 1400 K, confirmed by in-situ transformation of α- to γ-iron. Ultimately, the Fe and N_2 reacted uniformly throughout the beam path to form $Fe_3N_{1.33}$, as deduced from its established equation of state (EOS). We thus demonstrate that the activation energy provided by intense X-ray exposures in an XFEL can be coupled with the source time structure to enable exploration of time-dependence of reactions under high pressure conditions.

TOC GRAPHICS

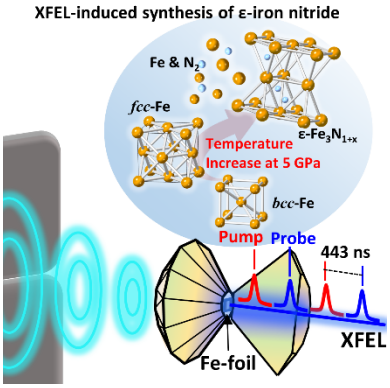

KEYWORDS X-ray free electron laser • Diamond-anvil cell • Solid-gas reaction • Iron • Iron nitride

Solid-gas reactions at high pressures and in high radiation environments are important in space and on (exo-) planets.[1] In such environments copious amounts of molecular nitrogen are found together with common refractory materials, such as iron alloys. On Earth, better understanding of the processes guiding to the evolution of atmospheric nitrogen on Earth, from its presence in a protoplanetary disc[2] to its present-day appearance in deep mantle reservoirs, is needed.[3,4]

In addition, recent theoretical work on solid-gas reactions such as Mg with Xe, Kr and Ar[5], iron and nickel with xenon[6], Kr with oxygen[7] and the possible formation of Helium compounds[8] warrants extensive exploratory synthesis efforts. The recent synthesis of a NiAr Laves phase[9] and $(Xe,Si)O_2$[10] supports changes of electronegativity at high pressures[11] and the opportunity to synthesize new materials with unusual properties.

High-pressure chemical synthesis is important since it permits the exploration of novel compounds at extreme conditions encountered in Earth and space science.[12] Diamond-anvil cell (DAC) experiments are suitable for such studies since the contained gas can function simultaneously as a pressure-transmitting medium (PTM) and a reactant. To trigger a chemical reaction, the energy of intense electromagnetic radiation pulses can be used.[13] Time-resolved diffraction and spectroscopic studies in a DAC at XFEL facilities have the potential to elucidate the formation and dynamics of new materials under extreme conditions.

Here we present an experimental setup using a DAC containing an Fe foil and N_2 as a PTM and reactant to demonstrate that a reaction to form ε-Fe_3N_{1+x} can be induced by appropriate XFEL pulse-probe conditions.

In addition to cosmochemical and planetary aspects,[14] iron nitrides have important technological applications due to their greater magnetization compared to iron oxides and lower manufacturing cost compared to iron alloys.[15,16] In general, iron nitrides are synthesized by

reacting Fe and NH_3 above 400 °C where Fe catalyzes the decomposition of ammonia. Atomic nitrogen then diffuses into bulk Fe with reaction times in the order of 100 seconds to form a nitride surface layer.[17] Our experiments here show that we can synthesize uniform ε-Fe_3N_{1+x} within nanoseconds without using conventional heating at an initial pressure of 5 GPa within a DAC. Previously, Hasegawa and Yagi synthesized Fe_2N using a laser heated DAC at pressures up to 10 GPa and temperatures near 1800 ± 50K.[18] Additional high-pressure and high-temperature syntheses of iron nitrides have led to the discovery of new Fe-N compounds such as α″-$Fe_{16}N_2$, α′-Fe_8N, γ′-Fe_4N, ε-Fe_3N_{1+x} ($-0.40 < x < 0.48$), Fe_7N_3, ζ-Fe_2N, γ‴-FeN, and most recently, Fe_3N_2, FeN_2 and FeN_4.[18-24] On the other hand, Laniel et al. revealed that after decompression of a laser-heated DAC to 5 GPa only Fe_2N was found, while above 17.7 GPa NiAs-type FeN was the most stable phase found after pressure release.[23] No indications for the presence of ε-Fe_3N_{1+x} was found in these studies up to pressures of 128 GPa. However, work by Clark et al. using ^{57}Fe-Mössbauer studies revealed a mixture of ζ-Fe_2N and ε-Fe_3N_{1+x} after laser heating at 1300 K below 10 GPa.[19]

Our experiments were performed at the High Energy Density (HED) instrument at the European X-ray Free Electron Laser (EuXFEL) facility in Schenefeld, Germany.[25-28] Pulses of 20 fs duration at 17.8 keV were generated in a train of 2-20 pulses at a 2.25 MHz repetition rate, repeating at 10 Hz. The fluence incident on the DAC at 100% transmission was 187(48) μJ/pulse over a spot size of 14 ± 1 μm FWHM, focused by the compound refractive lens (CRL), as measured using damage imprinting in freestanding Ta foil. At this repetition rate, XFEL pulses were so close in time (443 ns) that they may be used to pump and probe *in-situ* chemical reactions.[13,29]

A DAC with 500 μm culets was used as a pre-compression chamber. A small piece of a 4 μm thick Fe foil (< 250 μm × 250 μm, 99.99% purity) was loaded into a cylindrical chamber of 310 μm diameter and 50 μm height made by electro-spark erosion in a pre-indented rhenium gasket (Figure 1). A small spherical ruby crystal with ~10 μm diameter was placed into the sample chamber to determine the pressure.[30,31] We then loaded N_2 gas as a pressure transmitting medium (PTM) and a reactant using the gas loading system at the Extreme Conditions Science Infrastructure (ECSI) of PETRA III. The pressure of the sample inside the DAC was determined by recording the shift of the R1 emission line of ruby (precision: ± 0.1 GPa). The initial pressure of the sample before XFEL irradiation was set at 5.0(1) GPa. Prior to the experiment, the sample was characterized by synchrotron X-ray diffraction and optical techniques at the Extreme Conditions Beamline, P02.2, at PETRA III to confirm the presence of pure N_2 and Fe in the sample.

The horizontally polarized EuXFEL X-ray beam was directed along the central axis of the DAC, through both diamond culets (Figure 1). Powder X-ray diffraction patterns were collected at 10 Hz using two VAREX XRD4343 area detectors placed above and below the perpendicular direction of the XFEL beam (Figure 1). Patterns comprise a superposition of all scattering during each pulse train, allowing reactions to be tracked in a pump and probe fashion, while repeatedly exposing the sample. We recorded the X-ray diffraction pattern using different combinations of the XFEL fluence and pulses as summarized in Table 1. Dioptas software was used to convert 2-dimensional diffraction images to 1-dimensional diffraction patterns.[32] Following the *in- situ* XFEL measurements, *ex-situ* X-ray powder diffraction data of the reaction product were collected at the P02.2 beamline at PETRA III using a monochromatic synchrotron X-ray beam with 0.2898(1) Å wavelength and a Perkin Elmer XRD 1621 flat-panel detector. The incident X-

ray beam on the sample was focused to 2 μm FWHM beam using a pair of Kirkpatrick Baez (KB) mirrors. The CeO2 powder standard from NIST SRM 674b was used to calibrate the detector parameters using Dioptas. A 200 μm × 200 μm sample area was grid-scanned in 21 × 21 steps with 1 second exposure time per step.

Figure 2 shows photographic images of the sample before and after the XFEL experiments. Areas irradiated by the three different XFEL pump-and-probe modes are marked with A, B, and C (Table 1). While area A appears to be intact after exposure during run A (increasing pulse fluence), area B and C visibly show partial and complete alteration of the sample, after 20 consecutive pulses and continuous exposure with 2 consecutive pulses for 11 seconds, respectively. It should be noted that during exposure runs B and C, *in-situ* XRD patterns showed the presence of both the reaction product and compressed solid N_2 (Figure 3c). The observed damage on area C in Figure 2b is interpreted to result from the indirect effects of the X-ray absorption and heating in the sample leading to reaction.

Real-time changes in the X-ray diffraction patterns as a function of XFEL irradiation are summarized in Figure 3. First, we measured the XRD patterns using two consecutive pulses by changing the XFEL fluence to 10%, 30%, 50%, 70%, and 100%, (run A) to check the stability of the sample and the diamond anvil cell. In each two-pulse exposure, the first pulse probed the sample at ambient temperature and also increased its temperature as a result of the X-ray absorption. The second X-ray pulse probed the sample 443 ns after the first, measuring diffraction peaks that are shifted to lower q values, where the relative shift was used to estimate the temperature at this time (530 to 1424 K). The peak sample temperature was higher due to cooling between exposures, ranging from 700 K to 5700 K in the Fe for 10 to 100% transmitted power.[29]

As the XFEL fluence increased from 10 to 100 % transmission (~10^{10} to ~ 10^{11} photons per pulse), the diffraction peak intensities of the compressed solid N_2 and bcc-Fe (α-iron) increase as expected, which demonstrates that the anvils remain intact and maintain the original compression conditions (Figure 3a). At 30% transmission, a shoulder peak starts to form at the low-q side of the α-iron (110) peak, indicating an XFEL-induced thermal expansion. At 50% transmission, this shoulder peak grows and shifts further toward the low-q side, and above 70 % transmission, high-temperature fcc-Fe (γ-iron) is observed by the appearance of its (111) peak. The transformation of α- to γ-iron would require at least 900 K at 5 GPa.[33] Based on the refined peak positions and the established EOS of the iron phases,[34] we estimate residual temperatures of 750 and 1270 K at 50 and 70% fluence (2400 and 3900 K calculated peak temperatures), respectively (Figure 3a). The reaction between Fe and N_2, however, did not occur even at the full 100% transmission in run A, at which point the residual temperature is estimated to be 1424 K (5700 K peak temperature). The ~70% cooling between the pump and the probe is consistent with expectations for Fe samples.[29] The pulse to pulse energy variance of the XFEL, of order 30%, could lead to differing heating in shorter duration experiments, whereas in longer duration studies, where reactions products appear, only the averaged heating and duration is important. Thus, temperatures measured following single pulses (pump-probe) are consistent with expected values including initial volumetric X-ray absorption and heat transfer between pulses[29]; somewhat higher temperatures are expected after serial exposures in a MHz pulse train, due to heat accumulation[29], thus the temperature conditions reported following single pulses are lower bounds on those achieved after second and subsequent pulses in a train.

In contrast, XFEL-induced chemical reaction between Fe and N_2 is observed in the runs B and C (Figure 3a). The new peaks observed both *in-situ* and *ex-situ* after exposure during run B are

indexed as an ε-Fe_3N_{1+x} phase (Figure 3b). When we exposed the sample with serial XFEL trains for 11 seconds (run C), the formation of the ε-Fe_3N_{1+x} was observed from the third train by the growth of its (002) and (111) peaks (Figure 3c). In the first and second trains, we observed the growth of (111) and (002) Bragg reflections of fcc-Fe indicating temperatures of 1490 K and 1680 K, respectively. From the third train where ε-Fe_3N_{1+x} formed, the temperature was maintained between 1340 K and 1780 K up to the fourteenth train where the Bragg peaks of fcc-Fe disappeared. The ε-Fe_3N_{1+x} (and residual bcc-Fe) remained until the last train without any systematic changes in the relative peak intensities and positions. We estimate a cumulative absorbed energy of 3 mJ for the chemical reaction of Fe and N_2 at the pre-compression conditions of 5 GPa.

The sample pressure after run C increased to 7.8(1) GPa, where the unit cell parameters of ε-Fe_3N_{1+x} are refined to a = 4.707(1) Å and c = 4.357(1) Å in the space group $P6_322$ (no. 182) (Figure 3d). It is well established that the unit-cell volume of ε-Fe_3N_{1+x} is linearly proportional to the increasing nitrogen content x at ambient pressure.[35,36] The refined unit cell volume of the recovered ε-Fe_3N_{1+x}, e.g., 83.59(3) $Å^3$ at 7.8(1) GPa, would correspond to ε-Fe_3N_{1+x} with x = 0.33 at ambient conditions, assuming an EOS of B_0 = 172 GPa and B' = 5.7 as derived previously.[36] We therefore conclude that the composition of the XFEL-induced synthesis product is $Fe_3N_{1.33}$.

To investigate the cross-sectional textures and chemical distribution of the $Fe_3N_{1.33}$ reaction product, we have prepared the sample from run B using a focused Ga ion beam (FIB, 30 kV and 10 pA to 30 nA for surfacing) and performed scanning electron microscopy (SEM) (ZEISS Crossbeam 540 at Yonsei University) and scanning transmission electron microscope imaging (STEM, JEOL JEM-F200 combined with energy-dispersive X-ray spectroscopy) (Figure 4). The

sample was mounted on a Cu grid and measured in the annular dark-field mode. A two-dimensional elemental distribution of the cross-sectioned sample shown in Figure 4c and 4d reveal that over the 4 μm thickness of the original Fe-foil, the distribution of Fe and N appears to be uniform with regularly spaced holes representing degassed N_2 after the recovery of the sample. STEM data corroborate the results of the *in-situ* and *ex-situ* XRD by showing the distribution of the ABAB type stacking and distance between the Fe atoms, as expected for the ε-Fe_3N_{1+x} structure (Figure 4b). It is remarkable that such a homogeneous composition is obtained after such a short cumulative heating time as atomic nitrogen diffusion is in general a much slower process.[38]

In conclusion, our work demonstrates that the required activation energy for chemical reactions controlled by the XFEL radiation is an important experimental parameter. Despite only a limited number of exposures due to constraints and availability of in- and ex-situ characterizations we are confident that the XFEL parameters of our studies are well within parameters that are reproducible and in agreement with the known behavior of the Fe-N_2 system under high pressure and temperature. In contrast the kinetics of the XFEL-induced synthesis of ε-$Fe_3N_{1.33}$ are noteworthy and unprecedented. We found a remarkably homogeneous reaction product after the ultrafast reaction between Fe and nitrogen in a DAC at pressures above 5 GPa and temperatures exceeding 1400 K as pumped and probed by consecutive XFEL pulses separated by 443 ns. Following chemical reactions between gas and solid at high pressures and temperatures in a DAC using a tailored pump-probe setup at an XFEL open up a new parameter space for the exploration of new materials forming on fast timescales at high pressure.

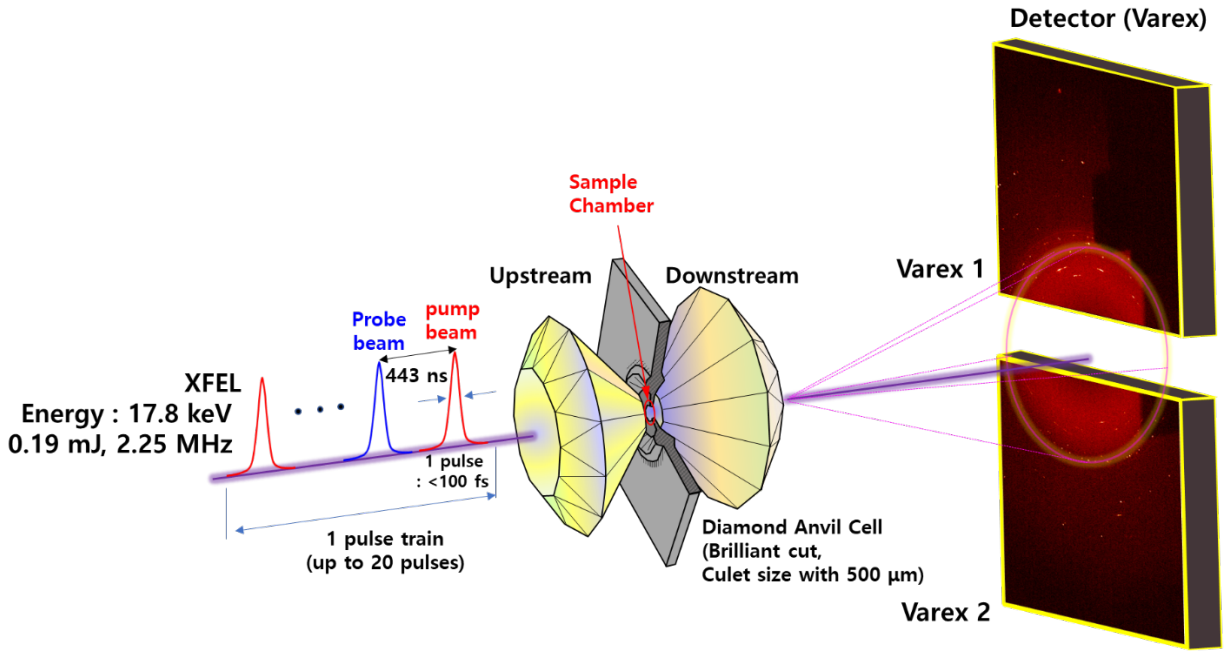

Figure 1. Experimental setup of the XFEL pump-and-probe using the DAC. Schematic diagram of the experimental setup at HED (High Energy Density science) Beamline at European XFEL.

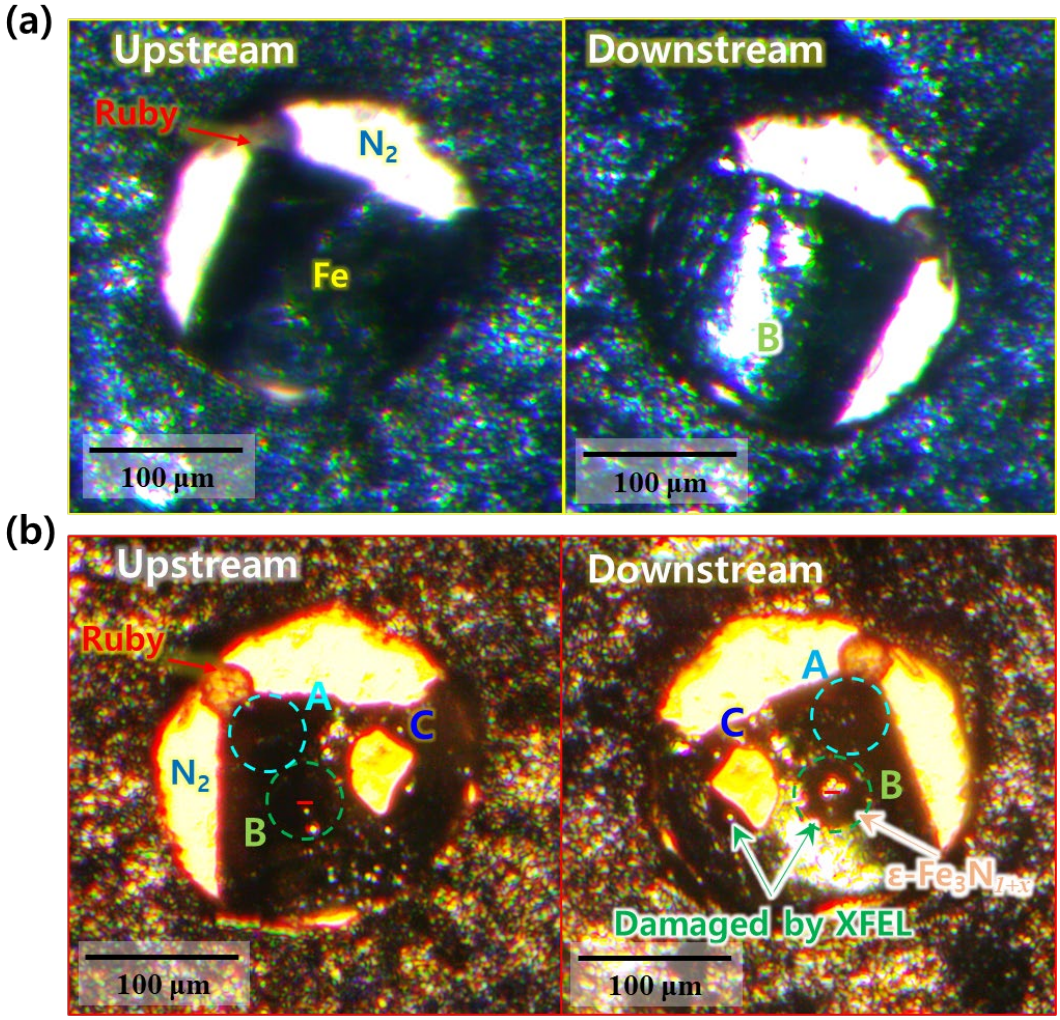

Figure 2. Photos of the sample inside DAC (a) before and (b) after a series of XFEL exposures as described in Table 1. The red line in (b) has been cross-sectioned by FIB for SEM and STEM imaging (see Figure 4).

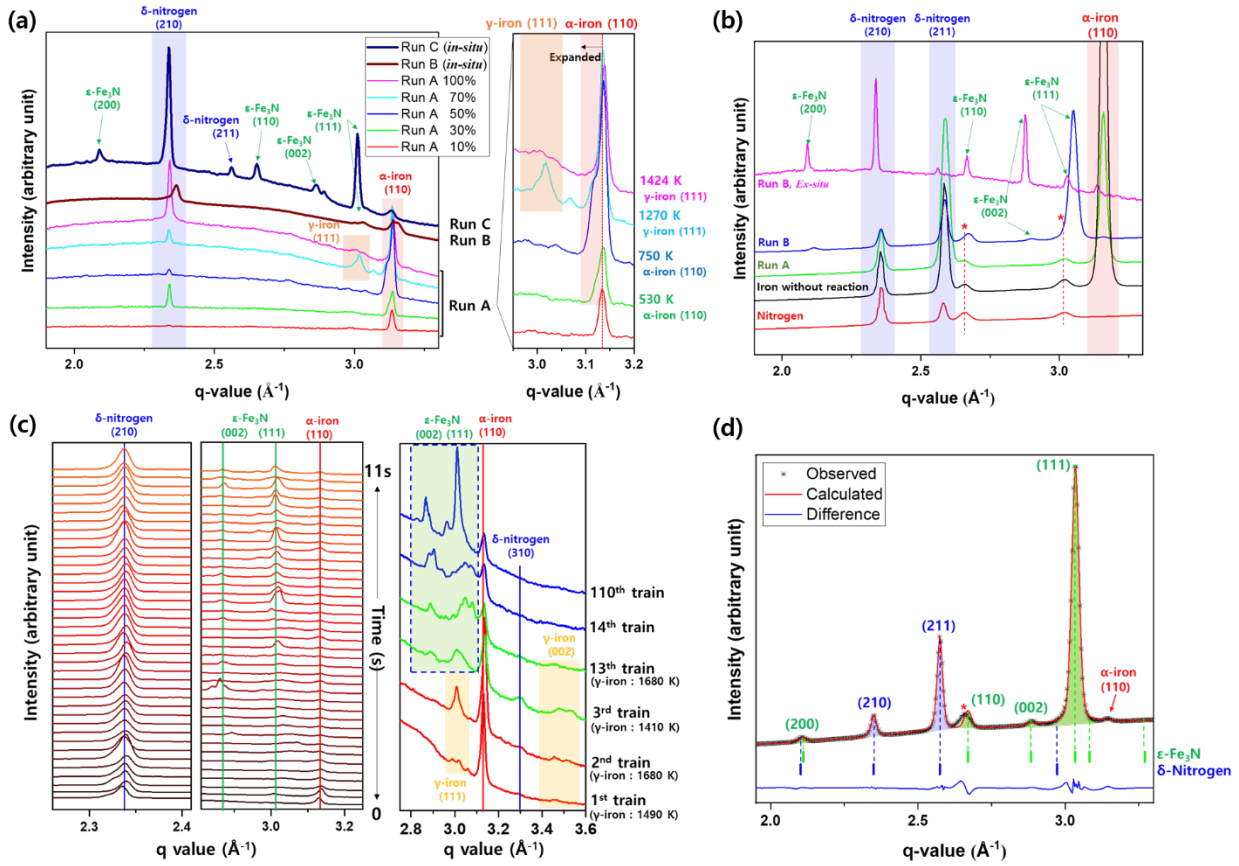

Figure 3. The changes of X-ray diffraction patterns of iron and nitrogen during and after in-situ chemical reaction by XFEL pump-and-probe. (a) Changes in diffraction patterns of the Fe foil under N_2 PTM pre-compressed to 5 GPa in a DAC. The percentages in run A indicate the transmission (fluence) of the XFEL. At 100% XFEL transmission, run B contains 20 consecutive pulses while run C has consecutive pulses over 11 seconds. (b) Synchrotron X-ray diffraction patterns collected at beamline P02.2 at PETRA III after run B, compared to the XFEL data measured right after run B (top pattern). After the XFEL experiments, the sample pressure has changed from 5.0(1) GPa to 7.8(1) GPa. (c) Changes in the diffraction patterns of the Fe foil during run C. (d) Profile fitting of the ex-situ XRD pattern measured after run B as shown in (b). ε-Fe_3N_{1+x} ($P6_322$) and δ-Nitrogen ($Pm\bar{3}n$) were fitted to an agreement index of R_{wp} = 1%. Observed data are shown in black crosses and the calculated pattern in a red line. Tick-marks under the pattern indicate the (hkl) reflection positions of the composing phases (green: ε-Fe_3N_{1+x}, blue: δ-Nitrogen). The red asterisk is an unidentified shoulder peak.

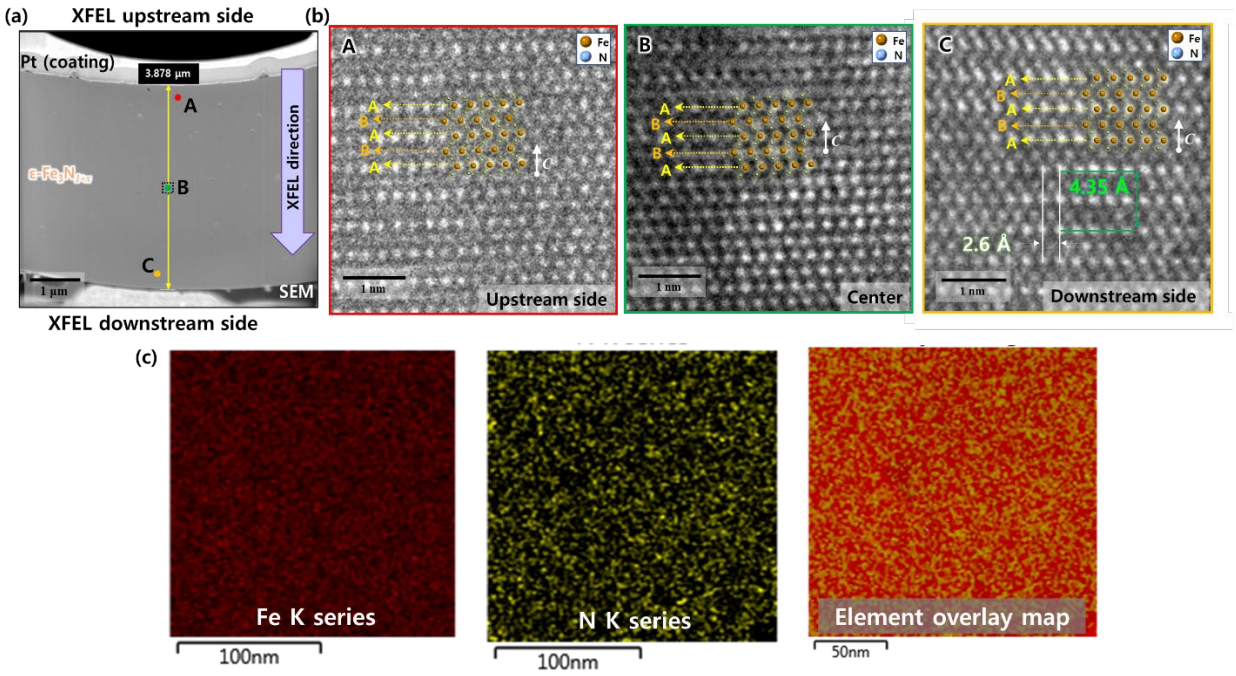

Figure 4. Electron microscope images and elemental mapping of the recovered sample. (a) A cross-sectional SEM image after exposure run B (the red line in Figure 2b). (b) The positions of the red, orange, and green area in the SEM image are shown by the STEM images. (c) Energy dispersive spectroscopy (EDS) elemental mapping of iron (left), nitrogen (middle), and their overlay (right) at the middle of the recovered sample (the green area in the SEM image).

Table 1. Pump and probe conditions used in our experiment.

Experimental run	XFEL pump and probe condition	
A	2.25 MHz 0.19 mJ/pulse 17.8 keV XFEL beam diameter: 14 μm ∅	With increasing XFEL transmission from 10 to 100 % (2 pulses per train)
B		20 consecutive pulses at 100% transmission (20 pulses in one train)
C		2 consecutive pulses per train at 100% transmission for 11 s (220 exposures)

ASSOCIATED CONTENT

AUTHOR INFORMATION

Corresponding Author

R. Stewart McWilliams − The School of Physics and Astronomy, Centre for Science at Extreme Conditions and SUPA, University of Edinburgh, Edinburgh, EH9 3FD, UK; E-mail: rs.mcwilliams@ed.ac.uk

Yongjae Lee − Department of Earth System Sciences, Yonsei University, Seoul 03722, Republic of Korea; E-mail: yongjaelee@yonsei.ac.kr

Notes

The authors declare no competing financial interests.

ACKNOWLEDGMENT

We thank H. Sinn for experimental assistance and T. Tschentscher and S. Pascarelli for fruitful discussions. This work was supported by the Leader Researcher program (NRF-2018R1A3B1052042) of the Korean Ministry of Sci-ence, ICT and Planning (MSIP). We also thank the supports by NRF-2019K1A3A7A09033395 and NRF-NRF-2016K1A4A3914691 grants of the MSIP. We acknowledge European XFEL in Schenefeld, Germany, for provision of X-ray free-electron laser beamtime at Scientific Instrument HED (High Energy Density Science) and would like to thank the staff for their assistance. The authors are indebted to the Helmholtz International Beamline for Ex-treme Fields (HIBEF) user consortium for the provision of instrumentation and staff that enabled this experiment. We acknowledge DESY (Hamburg,

Germany), a member of the Helmholtz Association HGF, for the provision of experimental facilities. Parts of this research were carried out at PETRA III (beamline P02.2). The research leading to this result has been supported by the project CALIPSOplus under the Grant Agreement 730872 from the EU Framework Program for Research and Innovation HORIZON 2020. Part of this work was performed under the auspices of the U.S. Department of Energy by Lawrence Livermore National Laboratory under Contract No. DE-AC52-07NA27344, and by the US Department of Energy through the Los Alamos National Laboratory, operated by Triad National Security, LLC, for the National Nuclear Security Administration (Contract No. 89233218CNA000001). Research presented in this article was supported by the by the Department of Energy, Labora-tory Directed Research and Development program at Los Alamos National Laboratory under project number 20190643DR and at SLAC National Accelerator Laboratory, under contract DE-AC02-76SF00515. Support is acknowl-edged from the Panofsky Fellowship at SLAC (awarded to EEM); the DOE Office of Fusion Energy Science funding num-ber FWP100182 (MF and EEM); EPSRC Grants EP/P024513/1 (RSM) and EP/R02927X/1 (EJP and MIM); the European Research Council (ERC) under the European Union's Horizon 2020 research and innovation Programme for grant agreements Nos. 670787 (GF, MAB, and GM) and 864877 (HM). KA, KG, RH, ZK, HPL, and RR thank the DFG for support within the Research Unit FOR 2440. SM and JC acknowledge support from the I-SITE ULNE project MetalCore (R-ERCGEN-19-006-MERKEL). CSY acknowledges DOE-NNSA (DE-NA0003342), NSF (DMR-1701360) and ARO (W911NF-17-1-0468).

REFERENCES

(1) Dawes, A.; Mason, N. J.; Tegeder, P.; Holtom, P. Laboratory Synthesis of Astrophysical Molecules. In : Electron Scattering From Atoms, Molecules (Eds.: Whelan, C. T.; Mason, N. J.), Springer, Boston, MA, 2005, pp. 329-340.

(2) Adler, J. F.; Willams, Q. A high-pressure X-ray diffraction study of iron nitrides : Implications for Earth's core. *J. Geophys. Res.* **2005**, 110, B01203

(3) Labidi, J.; Barry, P. H.; Bekaert, D. V.; Broadley, M. W.; Marty, B.; Giunta, T.; Warr, O.; Sherwood Lollar, B.; Fischer, T. P.; Avice, G.; Caracausi, A.; Ballentine, C. J.; Halldórsson, S. A.; Stefánsson, A.; Kurz, M. D.; Kohl, I. E.; Young, E. D. Hydrothermal $^{15}N^{15}N$ abundances constrain the origins of mantle nitrogen. *Nature* **2020**, 580, 367-371

(4) Mikhail, S.; Sverjensky, D. A. Nitrogen speciation in upper mantle fluids and the origin of Earth's nitrogen-rich atmosphere. *Nat. Geosci.* **2014**, 7, 816-819

(5) Miao, M.; Wang, X.; Brgoch, J.; Spera, F.; Jackson, M. G.; Kresse, G.; Lin, H.; Anionic Chemistry of Noble Gases : Formation of Mg-NG (NG = Xe, Kr, Ar) Compounds under Pressure. *J. Am. Chem. Soc.* **2015**, 137, 14122-14128

(6) Zhu, L.; Liu, H.; Pickard, C. J.; Zou, G.; Ma, Y. Reactions of xenon with iron and nickel are predicted in the Earth's inner core. *Nat. Chem.* **2014**, 6, 644-648

(7) Zaleski-Ejgierd, P.; Lata, P. M. Krypton oxides under pressure. *Sci. Rep.* **2016**, 6, 18938

(8) Liu, Z.; Botana, J.; Hermann, A.; Valdez, S.; Zurek, E.; Yan, D.; Lin, H.; Miao, M. Reactivity of He with ionic compounds under high pressure. *Nat. Commun.* **2018**, 9, 951

(9) Adeleke, A. A.; Kunz, M.; Greenberg, E.; Prakapenka, V. B.; Yao, Y.; Stavrou, E. A High-Pressure Compound of Argon and Nickel : Noble Gas in the Earth's Core? *ACS Earth Space Chem.* **2019**, 3, 2517-2524

(10) Crépisson, C.; Sanloup, C.; Blanchard, M.; Hudspeth, J.; Glazyrin, K.; Capitani, F. The Xe-SiO_2 System at Moderate Pressure and High Temperature. *Geochem. Geophys. Geosyst.* **2019**, 20, 992–1003.

(11) Rahm, M.; Cammi, R.; Ashcroft, N. W.; Hoffmann, R. Squeezing All Elements in the Periodic Table : Electron Configuration and Electronegativity of the Atoms under Compression. *J. Am. Chem. Soc.* **2019**, 141, 10253-10271

(12) Mao, H.-K.; Chen, B.; Chen, J.; Li, K.; Lin, J.-F.; Yang, W.; Zheng, H. Recent advances in high-pressure science and technology. *Matter Radiat. Extrem.* **2016**, 1, 59-75

(13) Pace, E. J.; Coleman, A. L.; Husband, R. J.; Hwang, H.; Choi, J.; Kim, T.; Hwang, G.; Chun, S. H.; Nam, D.; Kim, S.; Ball, O. B.; Liermann, H.-P.; McMahon, M. I.; Lee, Y.; McWilliams, R. S. Intense Reactivity in Sulfur-Hydrogen Mixtures at High Pressure under X-ray Irradiation. *J. Phys. Chem. Lett.* **2020**, 11(5), 1828-1834

(14) Adler, J. F.; Williams, Q. A high-pressure X-ray diffraction study of iron nitrides : Implications for Earth's core. *J. Geophys. Res.* **2005**, 110, B011203

(15) Zhang, Y.; Wang, Q. Magnetic-Plasmonic Dual Modulated FePt-Au Ternary Heterostructured Nanorods as a Promising Nano-Bioprobe. *Adv. Mater.* **2012**, 24,2485-2490

(16) Mahmoudi, M.; Shokrgozar, M. A. Multifunctional stable fluorescent magnetic nanoparticles. *Chem. Commun.* **2012**, 48,3957-3959

(17) Arabczyk W.; Pelka, R. Studies of the Kinetics of Two Parallel Reactions: Ammonia Decomposition and Nitriding of Iron Catalyst. *J. Phys. Chem. A* **2009**, 113, 411-416

(18) Hasegawa, M.; Yagi, T. Systematic study of formation and crystal structure of 3d-transition metal nitrides synthesized in a supercritical nitrogen fluid under 10 GPa and 1800 K using diamond anvil cell and YAG laser heating. *J. Alloy. Compd.* **2005**, 403, 131-142

(19) Clark, W. P.; Steinberg, S.; Dronskowski, R.; McCammon, C.; Kupenko, I.; Bykov, M.; Dubrovinsky, L.; Akselrud, L. G.; Sschwarz, U.; Niewa, R. High-Pressure NiAs-Type Modification of FeN. *Angew. Chem. -Int. Edit.* **2017**, 56, 7302, 7306

(20) Bykov, M.; Bykova, E.; Aprilis, G.; Glazyrin, K.; Koemets, E.; Chuvashova, I.; Kupenko, I.; McCammon, C.; Mezouar, M.; Prakapenka, V.; Liermann, H.-P.; Tasnádi, F.; Ponomareva, A. V.; Abrikosov, I. A.; Dubrovinskaia, N.; Dubrovinsky, L. Fe-N system at high pressure reveals a compound featuring polymeric nitrogen chains. *Nat. Commun.* **2018a**, 9, 2756

(21) Bykov, M.; Khandarkhaeva, S.; Fedotenko, T.; Sedmak, P.; Dubrovinskaia, N.; Dubrovinsky, L. Synthesis of FeN_4 at 180 GPa and its crystal structure from a submicron-sized grain. *Acta Cryst.* **2018b**, E74, 1392-1395

(22) Laniel, D.; Dewaele, A.; Anzellini, S.; Guignot, N. Study of the iron nitride FeN into the megabar regime. *J. Alloy. Compd.* **2018a**, 733, 53-58

(23) Laniel, D.; Dewaele, A.; Garbarino, G. High Pressure and High Temperature Synthesis of the Iron Pernitride FeN_2. *Inorg. Chem.* **2018b**, 57, 6245-6251

(24) Leineweber, A.; Jacobs., H.; Huning, F.; Lueken, H.; Schilder, H.; Kockelmann, W. ε-Fe_3N: magnetic structure, magnetization, and temperature dependent disorder of nitrogen. *J. Alloys Compd*. **1999**, 288, 79-87

(25) Mcwilliams, R. S. **2019**, DOI:10.22003/XFEL.EU-DATA-002292-00

(26) Decking, W. et al. A MHz-repetition-rate hard X-ray free-electron laser driven by a superconducting linear accelerator. *Nat. photonics*, **2020**, 14, 391-397

(27) Grünert, J.; Carbonell, M. P.; Dietrich, F.; Falk, T.; Freund, W.; Koch, A.; Kujala, N.; Laksman, J.; Liu, J.; Maltezopoulos, T.; Tiedtke, K.; Jastrow, U. F.; Sorokin, A.; Syresin, E.; Grebentsov, A.; Brovko, O. X-ray photon diagnostics at the European XFEL. *J. Synchrotron Rad.* **2019**, 26, 1422-1431

(28) Maltezopoulos, T.; Dietrich, F.; Freund, W.; Jastrow, U. F.; Koch, A.; Laksman, J.; Liu, J.; Planas, M.; Sorokin, A. A.; Tiedtke, K.; Grünert, J. Operation of X-ray gas monitors at the European XFEL. *J. Synchrotron Rad.* **2019**, 26, 1045-1051

(29) Meza-Galvez, J.; Gomez-Perez, N.; Marshall, A. S.; Coleman, A. L.; Appel, K.; Liermann, H. P.; McMahon, M. I.; Konôpková, Z.; McWilliams, R. S. Thermomechanical response of thickly tamped targets and diamond anvil cells under pulsed hard X-ray irradiation. *J. Appl. Phys*. **2020**, 127, 195902

(30) Mao, H. K.; Xu, J.; Bell, P. M. Calibration of the Ruby Pressure Gauge to 800 kbar Under Quasi-Hydrostatic Conditions. *J. Geophys. Res.* **1986**, 91, 4673-4676

(31) Dewaele, A.; Torrent, M.; Loubeyre, P.; Mezouar, M. Compression curves of transition metals in the Mbar range : Experiments and projector augmented-wave calculations. *Phys. Rev. B* **2008**, 78, 104102

(32) Prescher, C.; Prakapenka, V. B. DIOPTAS : a program for reduction of two-dimensional X-ray diffraction data and data exploration. *High Pressure Res.* **2015**, 35(3), 223-230

(33) Dewale, A.; Svitlyk, V.; Bottin, F.; Bouchet, J.; Jacobs, J. Iron under conditions close to the α–γ–ϵ triple point. *Appl. Phys. Lett.* **2018**, 112, 201906

(34) Dorogokupets, P. I.; Dymshits, A. M.; Litasov, K. D.; Sokolove, T. S. Thermodynamics and Equations of State of Iron to 350 GPa and 6000 K. *Sci. Rep.* **2017**, 7, 41863

(35) Guo, K.; Rau, D.; von Appen, J.; Prots, Y.; Schnelle, W.; Dronskowski, R.; Niewa, R.; Schwarz, U. High pressure high-temperature behavior and magnetic properties of Fe_4N : experiment and theory. *High Pressure Res.* **2013**, 33(3), 684-696

(36) Leineweber, A.; Jacobs, H.; Hüning, F.; Lueken, H.; Kockelmann, W. Nitrogen ordering and ferromagnetic properties of ϵ-Fe_3N_{1+x} ($0.10 \leq x \leq 0.39$) and ϵ-$Fe_3(N_{0.80}C_{0.20})_{1.38}$. *J. Alloy. Compd.* **2001**, 316, 21-38

(37) Niewa, R., Rau, D., Wosylus, A., Meier, K., Hanfland, M., Wessel, M., Dronskowski, R., Dzivenko, D. A., Riedel R. & Schwarz, U. High-Pressure, High-Temperature Single-Crystal Growth, Ab initio Electronic Structure Calculations, and Equation of State of ε-Fe_3N_{1+x}. *Chem. Mater.* **2009**, 21, 392-398

(38) Glasson, D. R.; Jayaweera, S. A. A. Formation and Reactivity of Nitrides. I. Review and Introduction. *J. Electrochem. Soc.* **1954**, 1010, 171-175